Multilayer Perceptron Equalizer for Optical Communication Systems

Tiago F. B. de Sousa* and Marcelo A. C. Fernandes†
Federal University of Rio Grande do Norte – UFRN
Department of Computer Engineering and Automation – DCA
Lagoa Nova, 59078-97, Natal-RN
Brazil
*tiagoair@dca.ufrn.br, †mfernandes@dca.ufrn.br

Abstract: Optical fibers are now widely used in communication systems, mainly because they offer faster data transmission speeds. Despite this great advantage, problems remain that prevent the full exploitation of optical connection: by increasing transmission rates over longer distances, the data is affected by nonlinear inter-symbol interference caused by dispersion phenomena. Adaptive equalizers can be used to compensate for the effects caused by nonlinear channel responses, restoring the signal originally transmitted. The present work proposes a multilayer perceptron equalizer based on artificial neural networks. The technique was validated using a simulated optical channel, and was compared with other adaptive equalization techniques.

Key–Words: Nonlinear optical signal processing, Dispersion compensation devices, Fiber optics communications, Neural networks.

1 Introduction

Optical fibers are the most commonly used data transmission system in high-speed networks, and are increasingly being implemented near the individual end-user. At first, because they use light to transmit data, it was believed that optical fibers had an infinite bandwidth, but with the increase in communication speeds, it became apparent that this was not the case, and it was observed that the quality of the received signal was affected by problems that had not previously been anticipated.

The difficulty with using such high speeds in optical fiber communications is the occurrence of inter-symbol interference (ISI), whose severity increases with the transmission distance. ISI in the fiber is mostly caused by two types of dispersion. The first is chromatic dispersion (CD), which is related to the fact that light waves propagate within the fiber at a speed that is dependent on their wavelength. CD increases with the square of the data transmission rate. The other type of dispersion is polarization mode dispersion (PMD), which is related to manufacturing defects, vibration, or mechanical stress of the optical fiber. Given the temporally variable nature of PMD, a means of adaptive compensation in the receiver is required [1].

At slow speeds, optical dispersion compensators may be practical and viable. However, as the speed increases, the cost becomes commercially unviable and electrical dispersion compensators are needed to reduce the problems of CD and PMD [2, 3]. These electrical dispersion compensators are generally adaptive equalizers, such as the linear transversal equalizer (LTE) or the decision-feedback equalizer (DFE), both trained with the least mean square (LMS) algorithm. However, CD and PMD associated with the photodiode (which converts light into electricity) induce nonlinear distortion in the transmitted signal, and these nonlinearities may distort the signal to an extent that cannot be compensated by a linear equalizer. One way around this problem is to use nonlinear adaptive equalizers that are able to filter nonlinear signals. An example is the neural equalizer that uses an artificial neural network to play the role of the adaptive equalizer. The use of electrical equalization in optical fiber communication systems is not new. Several techniques have been reported in the literature, including the use of LTE with LMS (LTE-LMS) [2], and the use of DFE to analyze the optimization criteria for the minimum bit error rate (mBER) [4]. Other approaches have used DFE with LMS (DFE-LMS) [3, 5, 6, 7, 8].

In the first proposals for neural equalizers (NE) using the multilayer perceptron (MLP) [9, 10, 11], it was observed that the process of equalization could be understood as a problem of artificial neural network (ANN) pattern classification. However, in these studies, only one-dimensional signals with 2-PAM modulation were used. Later studies proposed an ANN

with MLP for bi-dimensional signals [12, 13], using M-PAM and M-QAM modulations [14] and a modified version of the backpropagation (BP) algorithm for complex signals, presented in [15]. The approach adopted in this study involves a bi-dimensional neural equalizer with multilayer perceptron, trained with the backpropagation algorithm (BNE-MLP-BP), as originally proposed by [16, 17]. Instead of modifying the activation function to suit the complex domain, two neural networks are implemented, one to analyze the phase and the other to analyze the quadrature of the signal. In addition to avoiding the need to modify the activation function, this approach provided better results in terms of backpropagation algorithm training convergence, compared to the other procedures evaluated. The results are presented using bit error rate (BER) and training speed curves. In order to validate the proposed system, the BNE-MLP-BP equalizer was compared with the LTE-LMS and DFE-LMS equalizers.

2 Optical Communication Model

Figure 1 depicts an optical fiber communication system where the complex multilevel signal $a(n) = a(n)^I + j \cdot a(n)^Q$ is used to modulate the intensity of the laser (by signal $x(t)$), generating the modulated signal $g(t)$. In the fiber, the signal is subjected to chromatic and polarization mode dispersion effects, with output $u(t)$, and noise $n(t)$ is generated by the optical amplifiers. The term $n(t)$ (Amplified Spontaneous Emission noise or ASE noise) can be modeled as additive circularly symmetric, complex white Gaussian over the spectral bandwidth of the transmitted optical signal. Finally, the signal $z(t)$ passes through a photodetector that uses the squared modulus of the received signal to generate the electrical signal, $r(t)$, which is then equalized and sent to its destination .

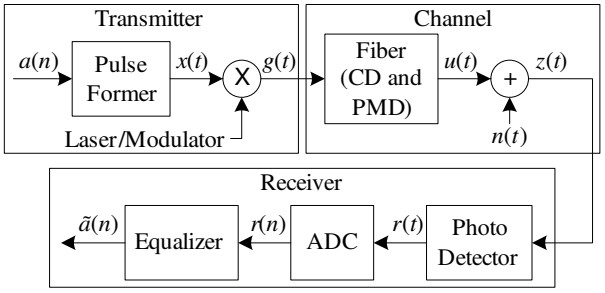

Figure 1: Optical communication system scheme.

2.1 Chromatic Dispersion

The transfer function of a channel with chromatic dispersion can be described by

$$H_{CD}(f) = e^{\left(\frac{j\pi DLf^2\lambda^2}{c}\right)}, \quad (1)$$

where f is the base band frequency of the signal, D is the chromatic dispersion constant of the fiber (also called material dispersion), L is the fiber length, λ is the signal wavelength and c is the speed of light [1, 2, 3].

2.2 Polarization Mode Dispersion

The transfer function of a channel with PMD can be expressed as

$$H_{PMD}(f, \tau, \alpha) = \sqrt{\alpha} e^{(-j\pi f\tau)}, \quad (2)$$

where f is the baseband signal frequency, α is the power splitting ratio (indicating the fraction of the total power that is projected into each polarization axis) and τ represents the Differential Group Delay (DGD) between the two polarization-axes [1] – [3].

2.3 Optical Channel Model

From the definitions reported previously [3, 5, 18, 19, 20, 21, 22], the optical channel can be modeled using the scheme shown in Figure 2 where $h_x(t)$ and $h_y(t)$ represent the CD and PMD impulse responses (in each polarization), $n_x(t)$ and $n_y(t)$ represent the ASE noise (in each polarization) due to the amplifiers, and $|(\cdot)|^2$ represents the non-linear effect of the photodetector.

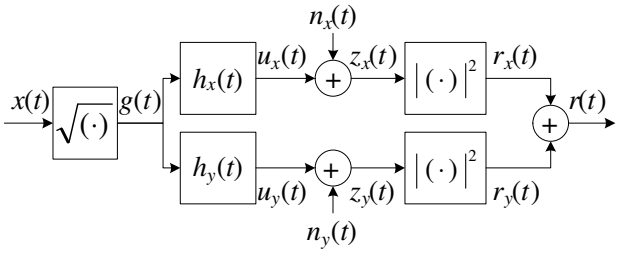

Figure 2: Optical channel model.

As reported in [3] and [19], the impulse response functions $h_x(t)$ and $h_y(t)$ can be represented by the expressions

$$\begin{aligned} h_x(t) &= F^{-1}\left(H_{CD}(f)H_{PMD}(f, \tau_x, \beta_x)\right) \\ &= \sqrt{\alpha}\sum_{k=0}^{N-1}\rho_k\delta(t - \tau_k - \tau_x) \end{aligned} \quad (3)$$

and

$$h_y(t) = F^{-1}\left(H_{CD}(f)H_{PMD}(f,\tau_y,\beta_y)\right) = \sqrt{1-\alpha}\sum_{k=0}^{N-1}\rho_k\delta(t-\tau_k-\tau_y) \quad (4)$$

where τ_x and τ_y represent the DGD of each polarization, α_x and α_y represent the fraction of the total power projected into each polarization, ρ_k is the k-th channel coefficient due to CD and N is the channel length. The coefficients ρ_k can be calculated using the expression presented in [3] and [19].

The output $r(t)$ is given by

$$r(t) = |u_x(t)+n_x(t)|^2 + |u_y(t)+n_y(t)|^2, \quad (5)$$

where

$$u_x(t) = \sqrt{\alpha}\sum_{k=0}^{N-1}\rho_k\sqrt{x\left(t-\tau_k-\tau_x\right)} \quad (6)$$

and

$$u_y(t) = \sqrt{1-\alpha}\sum_{k=0}^{N-1}\rho_k\sqrt{x\left(t-\tau_k-\tau_y\right)}. \quad (7)$$

3 Proposed Neural Equalizer

3.1 Architecture

Figure 3 illustrates the structure of the BNE-MLP-BP equalizer, which presents an architecture formed by two MLP networks. These networks, MLP-I and MLP-Q, operate in a parallel and independent way, so that each network is responsible for one dimension of the modulated signal. The MLP-I network processes the received signal in phase $r^I(n)$, while the MLP-Q network processes the received signal in quadrature, $r^Q(n)$.

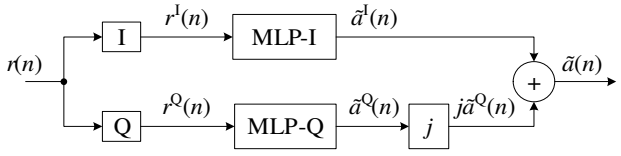

Figure 3: Bi-dimensional neural equalizer architecture.

The detailed architecture of the MLP-I and MLP-Q networks is similar to the structure presented in Figure 4, where $\tilde{a}^I(n)$ and $\tilde{a}^Q(n)$ are the estimates of the signals, $a^I(n)$ (phase signal) and $a^Q(n)$ (quadrature signal), respectively. In this study, the activation function of the hidden layer, $\varphi(\cdot)$, is a hyperbolic tangent function and the output layer function, $\phi(\cdot)$, is a linear function.

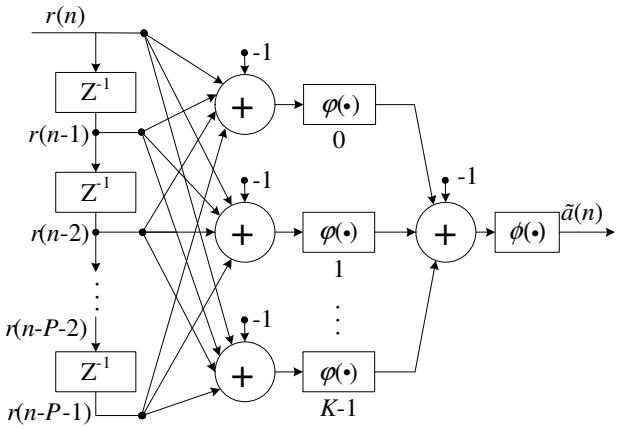

Figure 4: Neural equalizer architecture.

3.2 Training Schemes

Figures 5 and 6 illustrate two training schemes proposed for the BNE-MLP-BP equalizer. Both structures use two training modes, supervised and unsupervised [14].

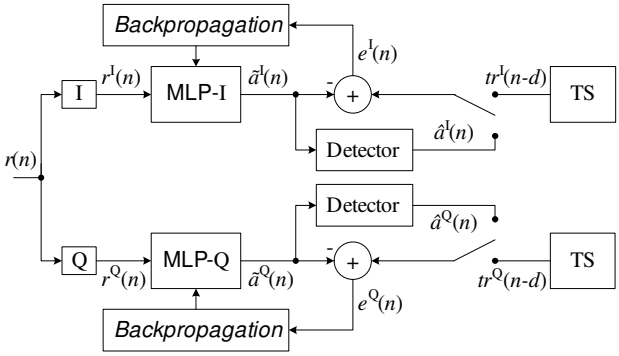

Figure 5: BNE-MLP-BP training scheme.

In the first structure, illustrated in Figure 5, the error signals $e(n)^I$ and $e(n)^Q$ are feedback directly to the BP algorithm. However, in the second scheme, proposed by [16] and illustrated in Figure 6, the error signal feedback to the symbols in phase and quadrature is composed of a joint error. For this reason the second proposal for the BNE-MLP-BP is called BNE-MLP-BP with Joint Error (BNE-MLP-BP-JE). A heuristic of integration between the MLP-I and MLP-Q networks is used for the joint error (JE), with

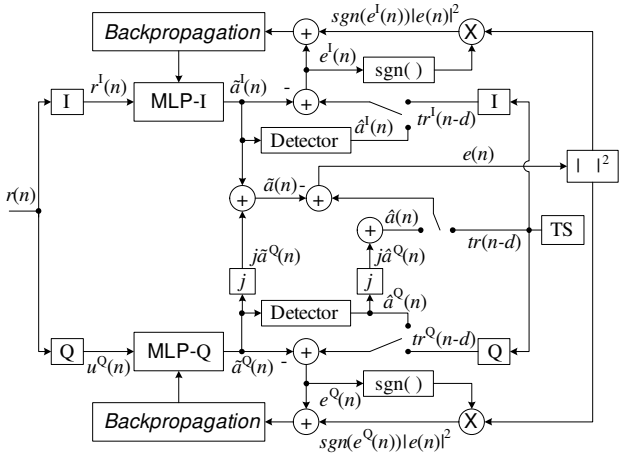

Figure 6: BNE-MLP-BP-JE training scheme.

the aim of increasing the convergence speed of the BNE-MLP-BP.

4 Simulations and Results

In order to validate the use of the BNE-MLP-BP equalizer in optical fibers, its performance and reliability were evaluated and compared with data obtained for the LMS adaptive equalizers (LTE and DFE) in a simulated environment.

Simulations were made for a 4-QAM digital modulation, with no channel encoders, using the optical channel model presented in Figure 2, with chromatic and polarization modal dispersions, which was simulated with two different fiber lengths. The parameters of the simulations are given in Table 1.

Table 1: Optical channel model parameters.

Parameters	Values
Bite rate	10 Gbps
Wavelength (λ)	1550 nm
Speed of light c	300000 km/s
Chromatic dispersion D	17 ps/nm-km
Fiber length L	50 and 100 km
Differential Group Delay (DGD)	200 ps
Power fraction (α) (for each axis of polarization)	1×10^{-3}

From the simulations, Bit Error Rate (BER) curves were plotted as a function of E_b/N_0 for each different fiber length value, in order to establish the relationship between bit energy and power spectral density. Learning curves with the Mean Square Error (MSE) were also employed to analyze the convergence time as a function of the quantity of frames transmitted. The constellations in the output of the equalizers were also acquired for the 4-QAM modulation, with E_b/N_0 of 30 dB. Table 2 presents the parameters used in the structures of the simulated equalizers.

Table 2: Parameters used in the simulated adaptive equalizers (50 and 100 km).

Structure	P	K	d	μ
FIR-LMS	64	–	16	0.001
DFE-LMS	32	–	16	0.01
BNE-MLP-BP	8	32	8	0.005
BNE-MLP-BP-JE	8	32	8	0.005

Figure 7 shows the performance curves for the simulations of the nonlinear optical communication channel described by Equation 5, with a fiber length of 50 km. As expected, LTE-LMS and DFE-LMS were unable to equalize the nonlinear optical channel, while, on the other hand, both the BNE-MLP-BP and the BNE-MLP-BP-JE equalizers showed satisfactory performance, with significant gains compared to the LMS equalizers.

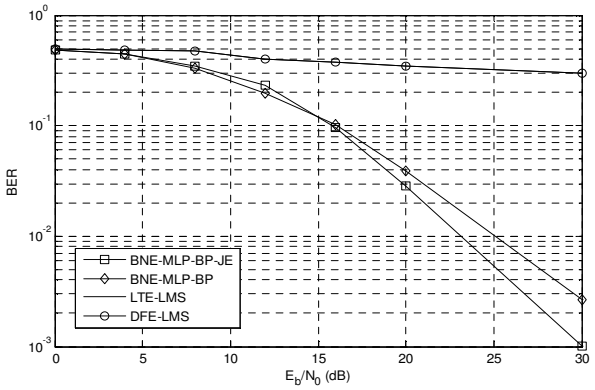

Figure 7: Performance curve of BER as a function of E_b/N_0 for the 4-QAM system (without channel coding), using the optical channel model presented in Figure 2 and fiber length of 50 km.

Analysis of the constellation at the output of the equalizers provides an indication of the substantial difference in performance between the LMS equalizers and the BNE-MLP-BP equalizer, using a signal-to-noise ratio of 30 dB. While BNE-MLP-BP could provide a visually recognizable constellation (Figures

8(c) and 8(d)), the DFE-LMS and LTE-LMS constellations were totally dispersed and unrecognizable (Figures 8(b) and Figure 8(a)).

In order to further evaluate the present proposal, the BNE-MLP-BP and BNE-MLP-BP-JE equalizers were also tested for a fiber length of 100 km. The LTE-LMS and DFE-LMS equalizers were not tested for this fiber length, due to their poor performance at the shorter length of 50 km. Table 2 presents the parameters of the equalizers used in the simulation with a fiber length of 100 km.

Figure 9 shows the BER curves obtained for the simulation with a fiber length of 100 km. It is important to note that even though the parameters for both networks were the same, the BNE-MLP-BP-JE equalizer outperformed the BNE-MLP-BP equalizer due to its joint error heuristic. Figures 10(a) and 10(b) show the constellations obtained for the BNE-MLP-BP and BNE-MLP-BP-JE equalizers.

With respect to the training curves for the simulation with fiber length of 50 km and 100 km (illustrated in Figure 11 and Figure 12) it was also observed that the performance of the BNE-MLP-BP and BNE-MLP-BP-JE equalizers were able to converge to lower error values, which didn?t happen with the LMS equalizers.

5 Conclusion

This paper presents the use of an ANN-based strategy, denoted BNE-MLP-BP, for the implementation of adaptive equalization. As the name implies, two MLP neural networks, MLP-I and MLP-Q, are used to perform equalization in the phase and the quadrature of the modulated signal. Two training schemes can be used. In the first scheme, the error is calculated independently for each network, while in the second scheme, the error is calculated using joint error heuristics. The BNE-MLP-BP equalizer was used in a simulated optical channel that exhibited the main problems related to optical fiber transmission. These were: chromatic and polarization mode dispersions, nonlinearities in the photoelectric converters, and influence of polarization occurring in the fiber itself, where there are two signal polarization modes, and a signal transmitted in one mode can affect the signal transmitted in the other mode. The simulations enabled the equalizers to be tested using different values of E_b/N_0, and to be compared with the classical LTE-LMS and DFE-LMS equalizers. BNE-MLP-BP proved to be effective in equalizing the channel, and showed significantly better performance than the classical techniques, especially at low SNR. It is therefore a valid system for use in the equalization of optical channels.

Acknowledgements: Financial support for this work was kindly provided by the Brazilian agency CAPES (Coordenação de Aperfeiçoamento de Pessoal de Nível Superior).

References:

[1] G. P. Agrawal, *Fiber-Optic Communication Systems*, 4th ed., ser. Wiley Series in Microwave and Optical Engineering. John Wiley and Sons, 2012.

[2] M. Kuschnerov, F. N. Hauske, L. Piyawanno, B. Spinnler, E. D. Schmidt, and B. Lankl, "Joint equalization and timing recovery for coherent fiber optic receivers," *ECOC 2008*, September 2008.

[3] J.-W. Park and W.-Z. Chung, "Performance analysis of electrical mmse linear equalizers in optically amplified ook systems," *J. Opt. Soc. Korea*, vol. 15, no. 3, pp. 232–236, Sep 2011.

[4] G. Katz and D. Sadot, "Radial basis function network equalizer for optical communication ook system," *Journal of Lightwave Technology*, vol. 25, no. 9, pp. 2631–2637, September 2007.

[5] J. Wang and J. M. Kahn, "Performance of electrical equalizers in optically amplified ook and dpsk systems," *IEEE Photonics Tech. Letters*, vol. 16, no. 5, pp. 1397–1399, 2004.

[6] J. Fickers, A. Ghazisaeidi, M. Salsi, G. Charlet, P. Emplit, and F. Horlin, "Decision-feedback equalization of bandwidth-constrained n-wdm coherent optical communication systems," *Lightwave Technology, Journal of*, vol. 31, no. 10, pp. 1529–1537, 2013.

[7] D. Zeolla, A. Antonino, G. Bosco, and R. Gaudino, "Dfe versus mlse electronic equalization for gigabit/s si-pof transmission systems," *Photonics Technology Letters, IEEE*, vol. 23, no. 8, pp. 510–512, 2011.

[8] J. Proesel, A. Rylyakov, and C. Schow, "Optical receivers using dfe-iir equalization," in *Solid-State Circuits Conference Digest of Technical Papers (ISSCC), 2013 IEEE International*, 2013, pp. 130–131.

[9] G. Gibson, S. Siu, and C. Cowan, "The aplication of nonlinear structures to the reconstruction

of binary signals," *Signal Processing*, vol. 39, no. 8, pp. 1877–1884, August 1991.

[10] S. Chen, G. J. Gibson, C. F. N. Cowan, and P. M. Grant, "Adaptive equalisation of finite nonlinear channels using multilayer perceptrons," *EURASIP Signal Processing Journal*, vol. 20, no. 2, pp. 107–119, February 1990.

[11] C. Cowan, "Nonlinear adaptive equalization [multilayer perceptron]," *Digital Processing of Signals in Communications*, pp. 1–5, September 1991.

[12] M. Peng, C. Nikias, and J. Proakis, "Adaptive equalization for pam and wam signals with neural networks," *Signals Systems and Computers*, vol. 1, pp. 496–500, November 1991.

[13] ——, "Adaptive equalization with neural networks: new multi-layer perceptron structures and their evaluation," *Acoustics, Speech and Signal Processing*, vol. 2, pp. 301–304, March 1992.

[14] J. Proakis, *Digital Communications*. McGraw-Hill Science/ Engineering/ Math, 2000.

[15] H.Leung and S. Haykin, "The complex backpropagation algorithm," *Signal Processing*, vol. 39, no. 9, pp. 2101–2104, September 1991.

[16] M. A. C. Fernandes, A. D. D. Neto, F. L. Garcia, and D. S. Arantes, "Equalização neural aplicada a sistemas com modulação digital bidimensional," *X Congresso Brasileiro de Inteligência Computacional*, Novembro 2011.

[17] T. F. B. de Souza and M. A. C. Fernandes, "Multilayer perceptron equalizer for optical communication systems," *st BRICS Countries Congress (BRICS-CCI) and 11th Brazilian Congress (CBIC) on Computational Intelligence*, September 2013.

[18] A. C. Singer, N. R. Shanbhag, and H.-M. Bae, "Electronic dispersion compensation: An overview of optical communications systems," *IEEE Signal Processing Magazine*, November 2008.

[19] K.-S. Kim, J.-H. Lee, W.-Z. Chung, and S.-C. Kim, "An electronic domain chromatic dispersion monitoring scheme insensitive to osnr using kurtosis," *J. Opt. Soc. Korea*, vol. 12, no. 4, pp. 249–254, Dec 2008.

[20] T. F. Portela, D. V. Souto, V. N. Rozental, H. B. Ferreira, and D. A. A. Mello, "Analysis of signal processing techniques for optical 112gb/s dp-qpsk receivers with experimental data," *Journal of Microwaves, Optoelectronics and Electromagnetic Applications*, vol. 10, no. 1, pp. 155–164, June 2011.

[21] M. Khafaji, H. Gustat, F. Ellinger, and C. Scheytt, "General time-domain representation of chromatic dispersion in single-mode fibers," *IEEE Photonics Tech. Letters*, vol. 22, no. 5, pp. 314–316, March 2010.

[22] S. J. Savory, "Digital filetrs for coherent optical receivers," *Optics Express*, vol. 16, no. 2, pp. 804–817, January 2008.

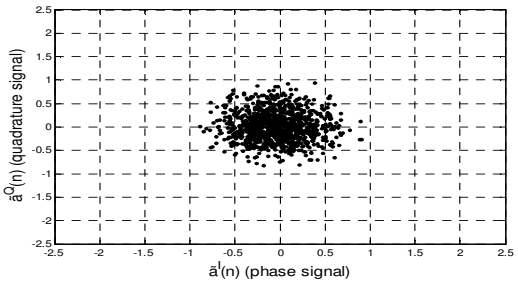

(a) LTE-LMS

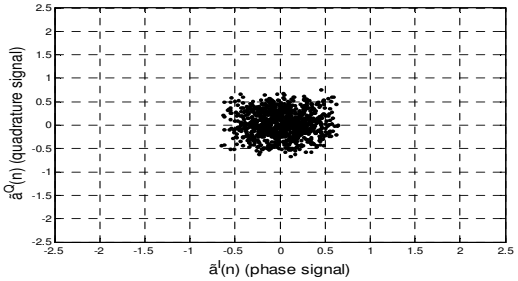

(b) DFE-LMS

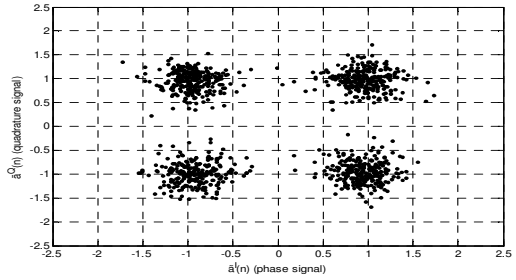

(c) BNE-MLP-BP

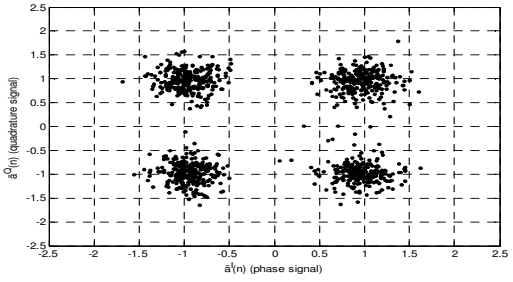

(d) BNE-MLP-BP-JE

Figure 8: Received signal constellations for the 4-QAM system (without channel coding), using the optical channel model presented in Figure 2, with $E_b/N_0 = 30$ dB and a fiber length of 50 km.

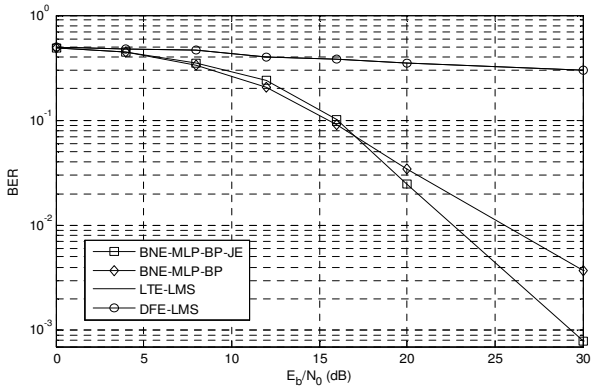

Figure 9: Performance curve of BER as a function of E_b/N_0 for the 4-QAM system (without channel coding), using the optical channel model presented in Figure 2, and a fiber length of 100 km.

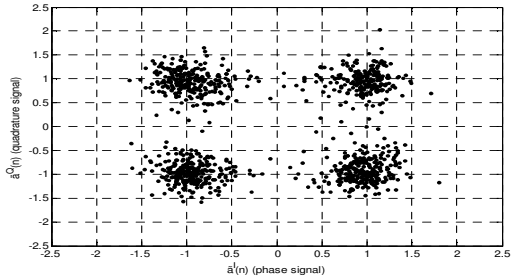

(a) BNE-MLP-BP

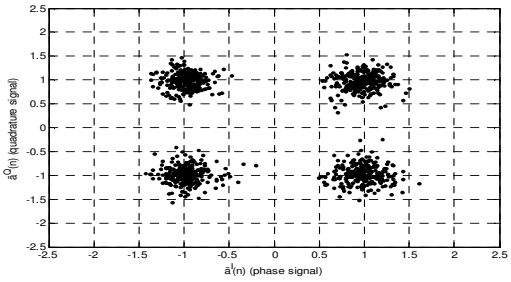

(b) BNE-MLP-BP-JE

Figure 10: Received signal constellations for the 4-QAM system (without channel coding) using the optical channel model presented in Figure 2 with $E_b/N_0 = 40$ dB and a fiber length of 100 km.

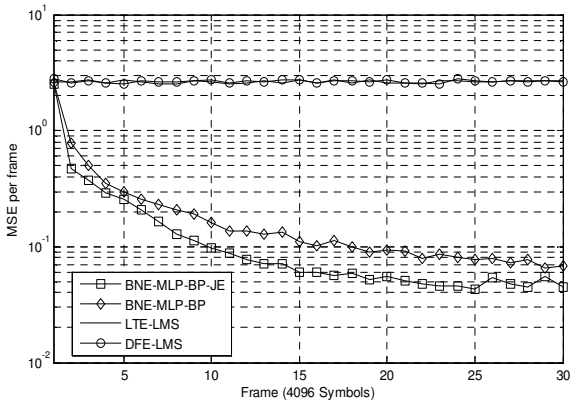

Figure 11: MSE curve for the 4-QAM system (without channel coding) using the optical channel model presented in Figure 2 with fiber length of 50 km and $E_b/N_0 = 30$ dB.

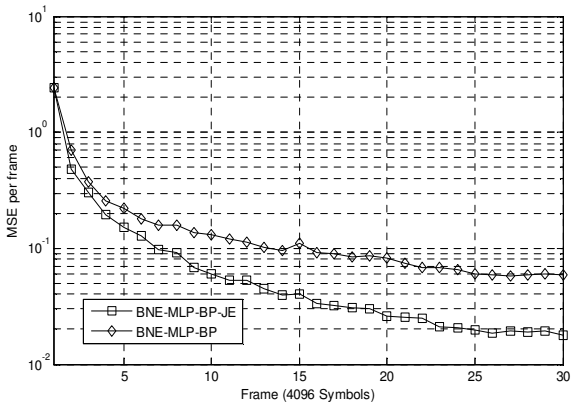

Figure 12: MSE curve for the 4-QAM system (without channel coding) using the optical channel model presented in Figure 2 with fiber length of 100 km and $E_b/N_0 = 30$ dB.